Few-Body Syst (2023) 64:21
https://doi.org/10.1007/s00601-023-01803-2

A. N. Hiller Blin · V. I. Mokeev

Polarized Proton Structure in the Resonance Region

Received: 14 March 2023 / Accepted: 3 April 2023 / Published online: 24 April 2023

Abstract In view of the precise data available on inclusive polarized electron scattering off polarized proton targets in the nucleon resonance excitation region, we compare these results with the coherent sum of resonant contributions to the polarized structure function g_1 and virtual photon asymmetry A_1. To this goal, we employ the nucleon resonance electroexcitation amplitudes determined for photon virtualities $Q^2 < 5.0$ GeV^2 from analyses of the CLAS data on exclusive electroproduction off protons in the resonance region. Most of the well established resonances of four star PDG status in the mass range up to 1.75 GeV are included. We find that the resonance-like structures observed in the inclusive g_1 data are related to the resonant contributions in the entire range of photon virtuality Q^2 where the data on g_1 are available. In the range of invariant mass of the final hadron system $W > 1.5$ GeV, the data on the asymmetry A_1 are well reproduced even when accounting for resonant contributions only, especially for the larger values of Q^2 and energies analysed. This observation offers an interesting hint to quark-hadron duality seen in polarized inclusive electron scattering observables.

1 Introduction

Inclusive electron scattering off protons and the exploration of its polarization observables offer an essential means to obtaining insights about the ground proton structure [1–3]. The extension of these studies to the resonance region will allow one to understand the proton structure at large values of the fractional parton momentum x in the resonance region and eventually to shed light on the strong interaction dynamics which underlies the transition from the strongly coupled to the perturbative QCD regimes, as well as the associated characteristics of quark-hadron duality [4–12].

There have been impressive advances in measuring inclusive scattering of polarized electron beams off polarized nucleon targets [13–20], which open the path to duality studies in spin-dependent observables [4,5,21–23]. In order to improve the theory approaches describing the connection between resonances and scaling contributions, considerations need to be made about the role of the nonresonant background. While such a quantitative description from first principles is rather challenging, insight may be obtained from phenomenological analyses.

A. N. Hiller Blin
Institute for Theoretical Physics, Tübingen University, Auf der Morgenstelle 14, 72076 Tübingen, Germany

A. N. Hiller Blin (✉)
Institute for Theoretical Physics, Regensburg University, 93040 Regensburg, Germany
E-mail: astrid.hiller-blin@itp.uni-tuebingen.de

V. I. Mokeev
Jefferson Lab, Newport News, VA 23606, USA

The experimental program exploring exclusive $\pi^+ n$, $\pi^0 p$, ηp, and $\pi^+\pi^- p$ electroproduction channels in the resonance region with the CLAS detector at Jefferson Lab has provided important new information on the $\gamma^* p N^*$ electrocouplings of most nucleon resonances in the mass range $W \leq 1.75$ GeV and for $Q^2 \leq 5$ GeV^2 [24–31]. These results allow one to quantitatively evaluate the coherent sum of resonant contributions to inclusive electron scattering observables, using parameters of the individual nucleon resonances extracted from data.

In our previous works [32–34], we confronted polarized and unpolarized inclusive electron-scattering data with the computation of resonant contributions in the resonance region. In the present work, we include updated data on the polarized structure function g_1 [20] and the virtual photon asymmetry A_1 [13–20]. In particular, the latter have extended the coverage in Q^2 and W in comparison with the data analyzed in our previous work, therefore permitting more insightful conclusions about the behavior of this observable in the resonance region.

In Sec. 2 we give a brief summary of the formalism, referring to our previous work [34] for a detailed description. The results of our computation compared with the available data are discussed in Sec. 3. In Sec. 4 we summarize our findings and give an outlook of these studies.

2 Formalism

The formalism used in the present work follows that thoroughly described in our previous article [34].

In terms of cross sections, the virtual photon asymmetries are given by [4,35,36]

$$A_1 = \frac{\sigma_T^{1/2} - \sigma_T^{3/2}}{\sigma_T^{1/2} + \sigma_T^{3/2}}, \qquad A_2 = \frac{\sigma_I}{\sigma_T}, \tag{1}$$

where σ_I is the real part of the interference amplitude for virtual photons with longitudinal and transverse polarizations. The structure functions are then related to the virtual photon asymmetries via

$$g_1 = \frac{1}{\rho^2} F_1 \Big(A_1 + A_2 \sqrt{\rho^2 - 1} \Big), \tag{2a}$$

$$g_2 = \frac{1}{\rho^2} F_1 \Big(- A_1 + \frac{A_2}{\sqrt{\rho^2 - 1}} \Big), \tag{2b}$$

with the kinematic factor $\rho^2 = 1 + Q^2/\nu^2$. Here, $-Q^2$ is the 4-momentum transfer squared between the electron and the proton, while ν is the virtual photon energy in the lab frame. It is related to the invariant mass W of the virtual photon–target proton system via $\nu = (W^2 - M^2 + Q^2)/2M$, where M is the nucleon mass.

The coherent sum of contributions from the resonances R to the inclusive structure functions can be written as [4,22]

$$\Big(1 + \frac{Q^2}{\nu^2}\Big) g_1^{\rm res} = M^2 \sum_{IJ\eta} \Bigg\{ \Bigg| \sum_{R^{IJ\eta}} G_+^{R^{IJ\eta}} \Bigg|^2 - \Bigg| \sum_{R^{IJ\eta}} G_-^{R^{IJ\eta}} \Bigg|^2 + \frac{\sqrt{2Q^2}}{\nu} \Re \Bigg[\Bigg(\sum_{R^{IJ\eta}} G_0^{R^{IJ\eta}} \Bigg) \Bigg(\sum_{R^{IJ\eta}} (-1)^{J_{R^{IJ\eta}} - \frac{1}{2}} \eta_{R^{IJ\eta}} G_+^{R^{IJ\eta}} \Bigg)^* \Bigg] \Bigg\}, \tag{3a}$$

$$\Big(1 + \frac{Q^2}{\nu^2}\Big) g_2^{\rm res} = -M^2 \sum_{IJ\eta} \Bigg\{ \Bigg| \sum_{R^{IJ\eta}} G_+^{R^{IJ\eta}} \Bigg|^2 - \Bigg| \sum_{R^{IJ\eta}} G_-^{R^{IJ\eta}} \Bigg|^2 - \frac{\nu\sqrt{2}}{\sqrt{Q^2}} \Re \Bigg[\Bigg(\sum_{R^{IJ\eta}} G_0^{R^{IJ\eta}} \Bigg) \Bigg(\sum_{R^{IJ\eta}} (-1)^{J_{R^{IJ\eta}} - \frac{1}{2}} \eta_{R^{IJ\eta}} G_+^{R^{IJ\eta}} \Bigg)^* \Bigg] \Bigg\}, \tag{3b}$$

for the spin-dependent structure functions, and

$$F_1^{\rm res} = M \sum_{IJ\eta} \Bigg\{ \Bigg| \sum_{R^{IJ\eta}} G_+^{R^{IJ\eta}} \Bigg|^2 + \Bigg| \sum_{R^{IJ\eta}} G_-^{R^{IJ\eta}} \Bigg|^2 \Bigg\}, \tag{3c}$$

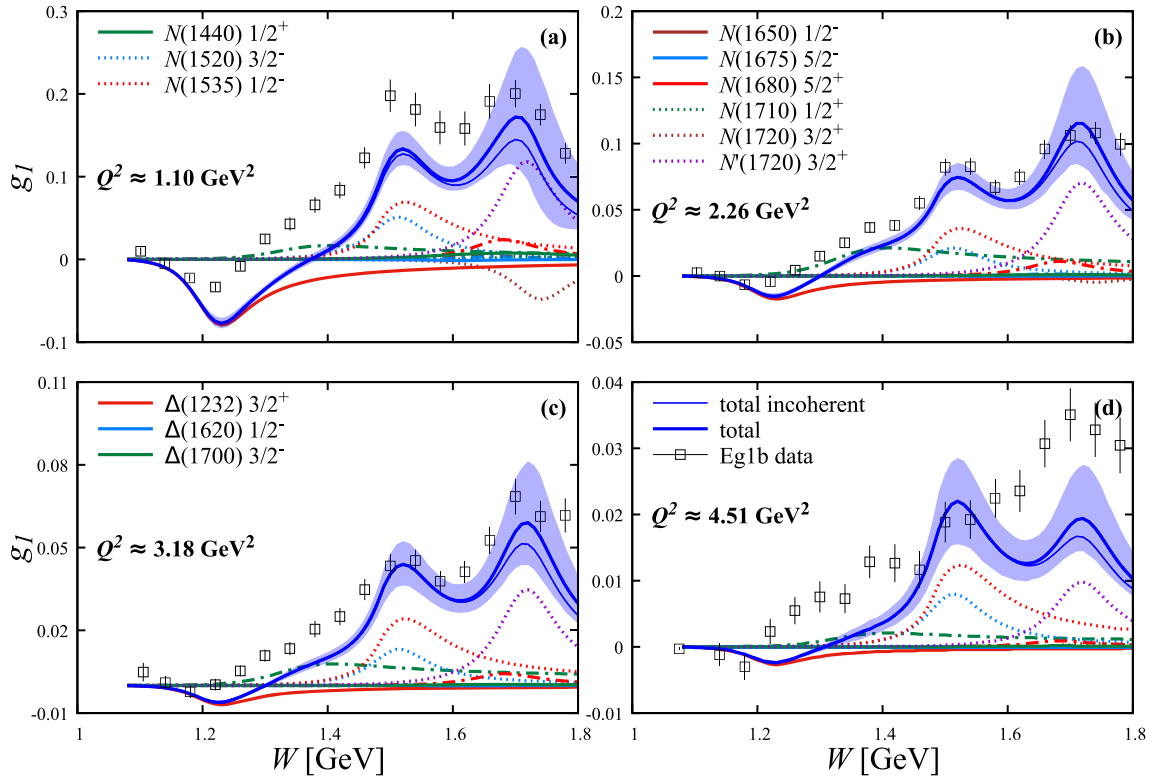

Fig. 1 Proton g_1 structure function data [20] (open black squares): **a** $Q^2 \approx 1.10$ GeV^2, **b** $Q^2 \approx 2.26$ GeV^2, **c** $Q^2 \approx 3.18$ GeV^2, **d** $Q^2 \approx 4.51$ GeV^2, compared to the coherent (thick blue curves) and incoherent (thin blue curves) sum of resonance contributions. The latter are computed at fixed Q^2 corresponding to the average value of the binned data in each panel. The contributions from individual N^* and Δ^* states are also shown separately. The uncertainties for the resonant contributions are computed by propagating the electrocoupling uncertainties via a bootstrap approach [32]

$$\left(1+\frac{\nu^2}{Q^2}\right)F_2^{\text{res}} = M\nu \sum_{IJ\eta}\left\{\left|\sum_{R^{IJ\eta}} G_+^{R^{IJ\eta}}\right|^2 + \left|\sum_{R^{IJ\eta}} G_-^{R^{IJ\eta}}\right|^2 + 2\left|\sum_{R^{IJ\eta}} G_0^{R^{IJ\eta}}\right|^2\right\}, \tag{3d}$$

for the spin-averaged structure functions. The outer sums in Eq. (3) run over the possible values of the spin J, isospin I, and intrinsic parity η, while the inner sums run over all resonances $R^{IJ\eta}$ that satisfy $J_R = J$, $I_R = I$ and $\eta_R = \eta$ for the spin, isospin and parity of the resonance R. The amplitudes G_+^R, G_-^R, and G_0^R describe the contribution from the electroexcitation amplitudes of the resonance R. They are related to the $\gamma^* pN^*$ electrocouplings $A_{1/2}$, $A_{3/2}$, and $S_{1/2}$ as detailed in Ref. [34]. The the $\gamma^* pN^*$ electrocouplings have become available from the studies of exclusive meson electroproduction data with the CLAS detector within the mass range of $W < 1.75$ GeV and for $Q^2 < 5.0$ GeV^2 [29,31,32,37].

3 Results

In Fig. 1, we compare the experimental results on the g_1 inclusive structure function measured with CLAS with the singled out resonant contributions, computed by employing resonance electroexcitation amplitudes deduced from exclusive CLAS electroproduction data [29,31,32,37]. This is outlined in Sec. 2. We constrain ourselves to the range of $W < 1.8$ GeV and $Q^2 < 5$ GeV^2 where the resonance electrocouplings are currently available. Both the individual resonance contributions, as well as the coherent and incoherent sums of resonances are shown. Since the fully inclusive structure function is given by resonant and non-resonant

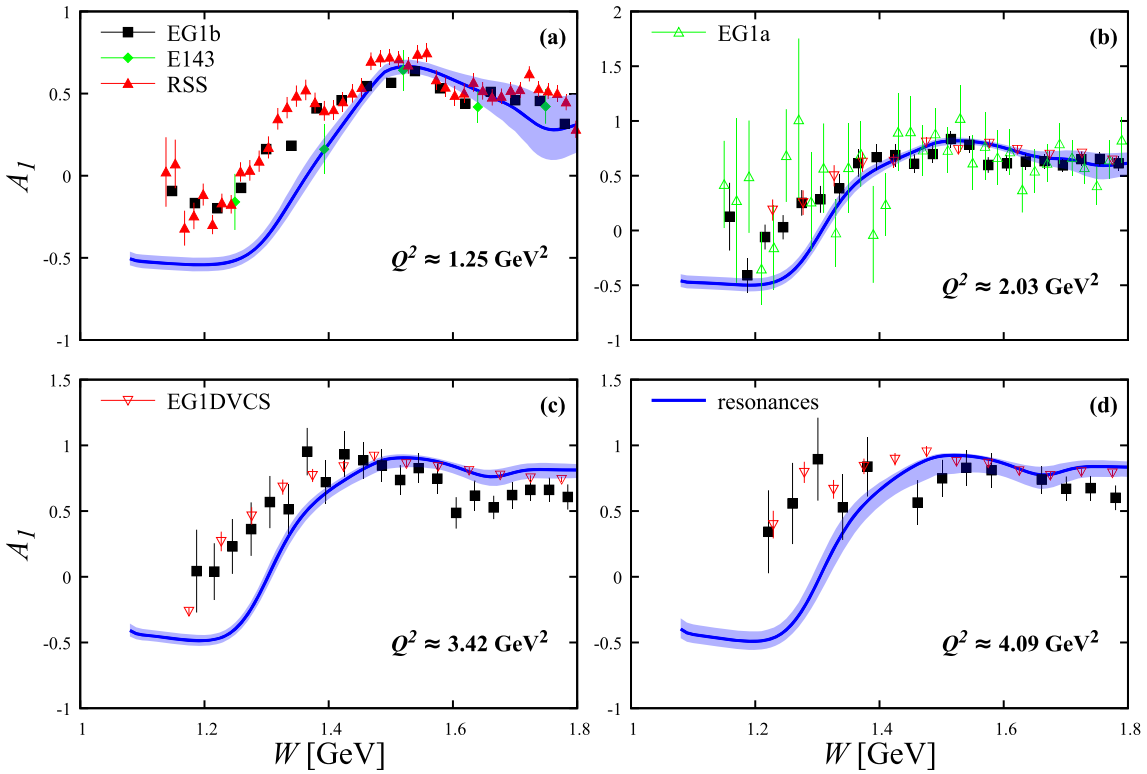

Fig. 2 A_1 asymmetry data from the E143 experiment at SLAC [13] (green filled diamonds), the RSS collaboration [17,18] (red filled triangles), as well as the CLAS experiments EG1a (green open triangles) [14], EG1DVCS (red open triangles) [19], and EG1b (black closed squares) [20]: **a** $Q^2 \approx 1.25$ GeV^2, **b** $Q^2 \approx 2.03$ GeV^2, **c** $Q^2 \approx 3.42$ GeV^2, **d** $Q^2 \approx 4.09$ GeV^2, compared to the computed purely resonant contributions (blue curves). The 1σ uncertainty bands of the resonant contributions are computed by propagating the electrocoupling uncertainties via a bootstrap approach [32]

contributions, we are able to explore the evolution of both contributions with W and Q^2. We find that non-resonant contributions in the third resonance region (1.6 GeV $< W <$ 1.8 GeV) increase with Q^2, indicating a transition to the partonic degrees of freedom in the ground proton state. Instead, in the second resonance region (1.4 GeV $< W <$ 1.6 GeV) the resonant contributions saturate the peak in the g_1 structure function. This points to the interplay between the resonant and non-resonant contributions, of interest for hadron structure theory. The rapid fall-off with Q^2 of the $\Delta(1232)3/2^+$ electroexcitation amplitudes makes the studies of g_1 in the first resonance region particularly sensitive to the non-resonant contributions, or to the ground nucleon parton behavior with fractional momenta x close to unity.

One can clearly see that the qualitative dips-and-peaks behavior in the W dependence of the inclusive data is accounted for by the resonant contributions, in all Q^2 bins. The dominant contribution in the first resonance region is that of the $\Delta(1232)\,3/2^+$, which in turn is driven by the G_- amplitude (or by the $A_{3/2}$ electrocoupling). According to Eq. (3), the contribution from the G_- amplitude squared enters g_1 with a minus sign. This explains the negative values seen both in the g_1 data around that peak, as well as in the purely resonant contributions. For most of the remaining states, it is the G_+ amplitude, related to the $A_{1/2}$ resonance electrocouplings, that dominates [32,34]. For this reason, the total resonant contributions to g_1 display a sign flip at W values between the first and second resonance peaks, as is also observed in the W-dependence of the measured g_1 data [20], as depicted in Fig. 1. Our analysis confirms that the resonance contributions are the drivers of this behavior.

In Fig. 2, we show the computed resonance contributions to the virtual photon asymmetry A_1, compared to the data measured both with the large-acceptance CLAS detector and with other detectors of smaller acceptance in the resonance region [13–20]. Since the asymmetry is defined by a cross-section ratio, the resonance structure becomes elusive.

Nevertheless, it is intriguing to find that, for $W > 1.5$ GeV, the W and Q^2 evolution of A_1 seen in the data is already rather well described by the inclusion of resonance contributions only. This points to a particular

sensitivity of the A_1 observable to the resonance contributions at $W > 1.5$ GeV. Such a behavior offers a hint for quark-hadron duality seen in this inclusive polarized electron scattering observable. This finding motivates the ongoing and future studies of resonance electrocouplings with the CLAS12 detector and a possible CEBAF energy increase up to 22 GeV [38], in order to scrutinize whether this behavior holds for even larger Q^2 values and for the higher-mass states.

In addition, the studies presented here can and have been extended to g_2 and A_2, therefore calling for future high-acceptance measurements of these observables.

4 Summary and Outlook

In these proceedings, we present the results on the exploration of the W and Q^2 dependence of the coherent and incoherent sums of nucleon resonance contributions to the spin-dependent g_1 structure function and the A_1 virtual-photon asymmetry. These are evaluated from the experimental results on $\gamma^* pN^*$ electrocouplings deduced from the analyses of exclusive meson electroproduction data. As input, we used the electroexcitation amplitudes extracted from CLAS data in the mass range up to $W = 1.75$ GeV [29,31,32,37].

Our findings provide evidence that the sign-flip behavior in the g_1 data is accounted for by the resonance contributions. In addition, the results point to a particular sensitivity of the A_1 observable to the resonant contributions at $W > 1.5$ GeV. This calls for further measurements at larger values of Q^2 and W, to investigate up to which QCD scales the resonant states remain sizeable and relevant.

Further, the need to confirm the findings in this work for g_2 and A_2 gives clear motivation for future large-acceptance measurements of these observables in experiments with polarized electron beams and for both longitudinal and transverse target polarizations.

The codes to generate the results presented in this article are available online [39].

Acknowledgements We thank S. Kuhn, V. Lagerquist, W. Melnitchouk, and P. Pandey for useful discussions and providing us with the experimental data shown here. This work was supported by the U.S. Department of Energy contract DE-AC05-06OR23177, under which Jefferson Science Associates, LLC operates Jefferson Lab, and by the Deutsche Forschungsgemeinschaft (DFG) through the Research Unit FOR 2926 (project number 409651613).

Funding Open Access funding enabled and organized by Projekt DEAL.

References

1. P. Jimenez-Delgado, W. Melnitchouk, J.F. Owens, J. Phys. G **40**, 093102 (2013). https://doi.org/10.1088/0954-3899/40/9/093102
2. J. Gao, L. Harland-Lang, J. Rojo, Phys. Rep. **742**, 1 (2018). https://doi.org/10.1016/j.physrep.2018.03.002
3. J.J. Ethier, E.R. Nocera, Ann. Rev. Nucl. Part. Sci. **70**, 43 (2020). https://doi.org/10.1146/annurev-nucl-011720-042725
4. W. Melnitchouk, R. Ent, C. Keppel, Phys. Rep. **406**, 127 (2005). https://doi.org/10.1016/j.physrep.2004.10.004
5. V. Lagerquist, S.E. Kuhn, N. Sato, arXiv preprint arXiv:2205.01218 (2022)
6. E.D. Bloom, F.J. Gilman, Phys. Rev. Lett. **25**, 1140 (1970). https://doi.org/10.1103/PhysRevLett.25.1140
7. M. Osipenko et al., Phys. Rev. D **67**, 092001 (2003). https://doi.org/10.1103/PhysRevD.67.092001
8. Y. Prok et al., Phys. Rev. C **90**(2), 025212 (2014). https://doi.org/10.1103/PhysRevC.90.025212
9. S.P. Malace et al., Phys. Rev. C **80**, 035207 (2009). https://doi.org/10.1103/PhysRevC.80.035207
10. M. Christy, P.E. Bosted, Phys. Rev. C **81**, 055213 (2010). https://doi.org/10.1103/PhysRevC.81.055213
11. V. Tvaskis et al., Phys. Rev. C **97**(4), 045204 (2018). https://doi.org/10.1103/PhysRevC.97.045204
12. Y. Liang et al., Phys. Rev. C **105**(6), 065205 (2022). https://doi.org/10.1103/PhysRevC.105.065205
13. K. Abe et al., Phys. Rev. D **58**, 112003 (1998). https://doi.org/10.1103/PhysRevD.58.112003
14. R. Fatemi et al., Phys. Rev. Lett. **91**, 222002 (2003). https://doi.org/10.1103/PhysRevLett.91.222002
15. P.E. Bosted et al., Phys. Rev. C **75**, 035203 (2007). https://doi.org/10.1103/PhysRevC.75.035203
16. K.V. Dharmawardane et al., Phys. Lett. B **641**, 11 (2006). https://doi.org/10.1016/j.physletb.2006.08.011
17. F.R. Wesselmann et al., Phys. Rev. Lett. **98**, 132003 (2007). https://doi.org/10.1103/PhysRevLett.98.132003
18. K. Slifer et al., Phys. Rev. Lett. **105**, 101601 (2010). https://doi.org/10.1103/PhysRevLett.105.101601
19. Y. Prok et al., Phys. Rev. C **90**(2), 025212 (2014). https://doi.org/10.1103/PhysRevC.90.025212

20. R. Fersch et al., Phys. Rev. C **96**(6), 065208 (2017). https://doi.org/10.1103/PhysRevC.96.065208
21. F.E. Close, F.J. Gilman, Phys. Rev. D **7**, 2258 (1973). https://doi.org/10.1103/PhysRevD.7.2258
22. C.E. Carlson, N.C. Mukhopadhyay, Phys. Rev. D **58**, 094029 (1998). https://doi.org/10.1103/PhysRevD.58.094029
23. J. Edelmann, G. Piller, N. Kaiser, W. Weise, Nucl. Phys. A **665**, 125 (2000). https://doi.org/10.1016/S0375-9474(99)00685-5
24. I.G. Aznauryan, V.D. Burkert, Prog. Part. Nucl. Phys. **67**, 1 (2012). https://doi.org/10.1016/j.ppnp.2011.08.001
25. I.G. Aznauryan et al., Phys. Rev. C **80**, 055203 (2009). https://doi.org/10.1103/PhysRevC.80.055203
26. V.I. Mokeev et al., Phys. Rev. C **86**, 035203 (2012). https://doi.org/10.1103/PhysRevC.86.035203
27. V.I. Mokeev et al., Phys. Rev. C **93**(2), 025206 (2016). https://doi.org/10.1103/PhysRevC.93.025206
28. K. Park et al., Phys. Rev. C **91**, 045203 (2015). https://doi.org/10.1103/PhysRevC.91.045203
29. D.S. Carman, K. Joo, V.I. Mokeev, Few Body Syst. **61**(3), 29 (2020). https://doi.org/10.1007/s00601-020-01563-3
30. V.I. Mokeev et al., Phys. Lett. B **805**, 135457 (2020). https://doi.org/10.1016/j.physletb.2020.135457
31. V.D. Burkert, arXiv:2212.08980 [hep-ph] (2022)
32. A.N. Hiller Blin et al., Phys. Rev. C **100**(3), 035201 (2019). https://doi.org/10.1103/PhysRevC.100.035201
33. A.N. Hiller Blin, W. Melnitchouk, V.I. Mokeev, V.D. Burkert, V.V. Chesnokov, A. Pilloni, A.P. Szczepaniak, Phys. Rev. C **104**(2), 025201 (2021). https://doi.org/10.1103/PhysRevC.104.025201
34. A.N. Hiller Blin, V.I. Mokeev, W. Melnitchouk, Phys. Rev. C **107**, 035202 (2023). https://doi.org/10.1103/PhysRevC.107.035202
35. R.G. Roberts, *The Structure of the Proton: Deep Inelastic Scattering* Cambridge Monographs on Mathematical Physics. (Cambridge University Press, Cambridge, 1990). https://doi.org/10.1017/CBO9780511564062
36. K. Dharmawardane, Spin Structure Functions of the Deuteron Measured with CLAS in and above the Resonance Region. Ph.D. thesis, Old Dominion U. (2004). DOI: https://doi.org/10.2172/824941
37. V.I. Mokeev, D.S. Carman, Few Body Syst. **63**(3), 59 (2022). https://doi.org/10.1007/s00601-022-01760-2
38. P. Achenbach, et al., arXiv:2303.02579 [hep-ph] (2023)
39. Codes to generate reonance contributions to inclusive electron-proton scattering observables. https://github.com/astridhillerblin/SFRes